# Thermal training of exchange bias in epitaxial Fe/$KNiF_3$

L. Wee and R. L. Stamps*
*School of Physics, M013, University of Western Australia, 35 Stirling Highway, Crawley, Western Australia 6007, Australia*

L. Malkinski and Z. Celinski
*Department of Physics, University of Colorado, Colorado Springs, Colorado 80918, USA*

D. Skrzypek
*Institute of Physics, University of Silesia, Uniwersytecka 4, Katowice 40-007, Poland*
(Received 19 May 2003; published 29 April 2004)

Shifted hysteresis loops and enhanced coercivities associated with the phenomena of exchange bias were examined experimentally for a model system. Superconducting quantum interference device magnetometry measurements are discussed for bilayer structures, consisting of single-crystal Fe(001) and $KNiF_3$ films grown in ultrahigh vacuum. The structures were characterized using reflection high-energy electron diffraction and x-ray diffraction. The $KNiF_3$ film structure was either single crystal or polycrystalline with a high degree of texture. The interfaces are expected to be fully compensated for this particular growth orientation, and good lattice match between the ferromagnetic and antiferromagnetic layers preserved the cubic structure of both. An exchange bias shift was observed and coercivities were enhanced for temperatures well below the Neél temperature. Features associated with training were exhibited by this epitaxial system and clear evidence of thermally activated processes for single-crystal films were obtained in a thermal pulse experiment. Possible evidence for two types of energy barrier distributions controlling the magnetization process is presented. The existence of training and its correlation with thermal activation processes suggest that exchange bias in this mainly compensated system is controlled by magnetization processes in the antiferromagnet. Spin-flop coupling is very likely in this system, and it is suggested that pinning of antiferromagnet spins near the interface is responsible for the exchange bias shifts.

DOI: 10.1103/PhysRevB.69.134425 PACS number(s): 75.70.Cn, 75.60.Nt, 81.15.Hi, 68.35.Ct

## I. INTRODUCTION

The distinct magnetic properties of a ferromagnet-antiferromagnet interface and of the antiferromagnet itself were recognized from the beginning as key elements associated with exchange bias.[1–4] Over the four decades since its discovery, a number of mechanisms have been proposed and explored in order to explain behavior observed through experiments on a huge variety of systems. There is a large literature on past experimental and theoretical work, and extensive references can be found in several recent reviews.[5–8]

The importance of understanding exchange bias has increased in recent years due to the potential for using this effect to engineer magnetic structures with desired anisotropic pinning features. On a more fundamental level, the ability to grow and study metallic and insulating magnetic thin films with atomic level precision has allowed for new studies of enduring problems related to exchange bias. These studies have been facilitated by advances in structural and magnetic characterization techniques, which have seen considerable improvement in scope and sensitivity over the past decade.[9,10]

In this paper experimental results are presented for an epitaxially grown bilayer designed as a model system for studying exchange bias at compensated interfaces. The system consists of a $KNiF_3$ film grown onto a single-crystal Fe film, prepared using molecular-beam epitaxy (MBE). $KNiF_3$ is thought of as a model Heisenberg antiferromagnet and much is known of its low-temperature high-frequency properties.[11] An important feature of this particular cubic perovskite is that a single-crystal $KNiF_3$ film with its [001] axis directed normal to the interface can be grown on single-crystal Fe. The interface is magnetically compensated in this orientation since both antiferromagnet sublattices are present at the interface.[12–14]

The existence of exchange bias at ideally compensated interfaces has been discussed by a number of authors.[15–19] Several conditions have been identified for exchange bias to exist. A basic requirement is for there to be a mechanism for uncompensated exchange coupling between the ferromagnet and the antiferromagnet through the interface. This can occur with significant spin-flop coupling[15] at the interface, thereby providing a magnetic moment at an otherwise compensated antiferromagnetic layer of spins. If the canted moment is somehow maintained throughout a magnetization loop (either through additional in-plane magnetocrystalline anisotropies or pinned as a consequence of disorder or impurity induced local pinning fields), irreversible bias may occur. A significant bias shift then requires an antiferromagnetic film thick enough to support a large antiferromagnetic domain.[19] The magnitude of the bias shift will also be affected by the possible formation of a ''twist'' in the antiferromagnet, as suggested by Mauri *et al.*[20] Crystalline defects at the interface and geometric roughness can also create regions of uncompensated antiferromagnet interface, and thereby generate an exchange bias loop shift.[21] Mixed interface models that include contributions simultaneously from both compensated and uncompensated regions show characteristic effects on

 

hysteresis loop shape, angular dependence of bias field magnitude, and coercivity.[8,22,23]

A strong dependence on exchange bias in the Fe/$KNiF_3$ system on interface quality can therefore be expected. Furthermore, in the simplest approximation, the magnitude of the bias field should scale as a product of antiferromagnetic film thickness and magnetic anisotropy field. However bulk $KNiF_3$ is known to have a very small magnetocrystalline anisotropy, and due to the good lattice match between the Fe and $KNiF_3$,[24] crystal strains should be small at the interface. Hence the effective anisotropy field of the antiferromagnet should be close to its bulk value, which is on the order of several tens of Oersteds. The conclusion is that significant bias shifts can only be expected for thick $KNiF_3$ films.

This paper provides a detailed account of the growth and structural characterization of Fe/$KNiF_3$ bilayers. In previous papers, we have reported on the magnetization and high-frequency behavior of a small subset of these samples, and compared these properties at room and at cryogenic temperatures.[25,26] In the present paper, the temperature dependence of the bias magnitudes and coercive fields is examined for a full range of samples including a number of different crystalline qualities and $KNiF_3$ thicknesses.

A blocking temperature significantly smaller than $T_N$ is found over the entire range of samples. Enhanced coercivities are also observed at low temperature, in some cases persisting up to $T_N$. The most surprising feature reported in the present work is training effects found for single-crystal samples and results are presented from thermal pulse experiments that shed light on the origin of these effects. This method was used to demonstrate that the training is due to thermal activation processes in the antiferromagnet.

The remainder of this paper is organized as follows. Sample growth and characterization are described in the following section, along with details of the magnetometry experiments. Exchange bias shifts of the hysteresis curve and features of the coercivity are discussed in Sec. III, with particular attention to features appearing in the magnetization measurements due to the use of a Fe seed layer during growth. The temperature dependence of bias and coercive fields is also described in this section. Section IV contains details of the training and heat pulse experiments. The results and conclusions are summarized in the final section.

## II. GROWTH OF EPITAXIAL BILAYERS

### A. Sample preparation

Bilayers of Fe/$KNiF_3$ were grown in an ultrahigh vacuum MBE system using thermal cells and electron-beam evaporators, and the base pressure was maintained at about $10^{-9}$ torr throughout the growth process. The structures were grown on GaAs(001) substrates which were carefully prepared by repeated cycles of sputtering and high-temperature annealing. This procedure resulted in a Ga-terminated surface, with some samples showing evidence of surface reconstruction by characteristic streaks in its reflection high-energy electron diffraction (RHEED) pattern. A thin Fe seed layer was first deposited directly onto the substrate, followed by a 50–70 nm Ag template. The structure was annealed at 620 K for at least 24 h to improve surface smoothness and crystallinity prior to growth of the main Fe film. The $KNiF_3$ was grown using a 6 kV *e*-beam source with a low emission current of 3 mA. A capping layer of Au was deposited before the sample was exposed to ambient conditions for measurements. A sketch of the sample structure is shown in Fig. 1.

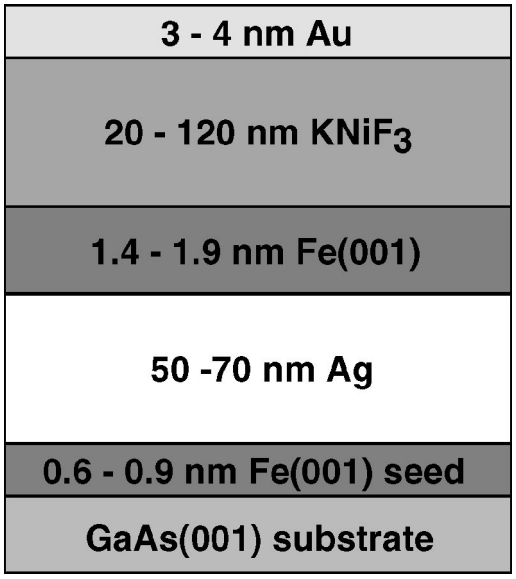


FIG. 1. Schematic diagram of the studied structures. The Fe/$KNiF_3$ bilayers were grown on a (001)-oriented GaAs substrate with Fe seed layer and Ag template. The structures were capped with Au for protection prior to measurements at ambient conditions.

### B. Structural characterization

Growth of the Fe and $KNiF_3$ films was monitored *in situ* by RHEED. The Fe grew as a single crystal with its [001] axis normal to the surface, and oriented in plane with the Fe[100] easy anisotropy axis along the $KNiF_3$[110] hard axis.[13] Quasi-layer-by-layer growth of the Fe film was observed, at least for some portion of the growth process, as evidenced by RHEED intensity oscillations.[27]

RHEED analysis on completed $KNiF_3$ films showed polycrystalline structure in some samples. Single-crystal or two-phase bicrystalline $KNiF_3$ structure was clearly shown in three samples for which the substrate temperature had been elevated during growth. Fully single-crystal samples were indicated by distinct spots on the RHEED pattern indexable to principal low-order crystallographic planes. In bicrystalline films, multiple diffraction spots were observed for each plane, suggesting a highly textured structure containing some degree of crystallite misorientation.

RHEED patterns showing the range in crystalline quality are given in Fig. 2. In (a), the RHEED pattern is for a polycrystalline $KNiF_3$ film, and in (b) the pattern for a single-crystal $KNiF_3$ film is shown. *Ex situ* x-ray analysis using a Scintag XDS2000 diffractometer on polycrystalline $KNiF_3$ test films grown directly onto GaAs revealed diffraction peaks indexed to stoichiometric $KNiF_3$ with an approximate grain size of 11 nm (see Fig. 3). The incident beam was

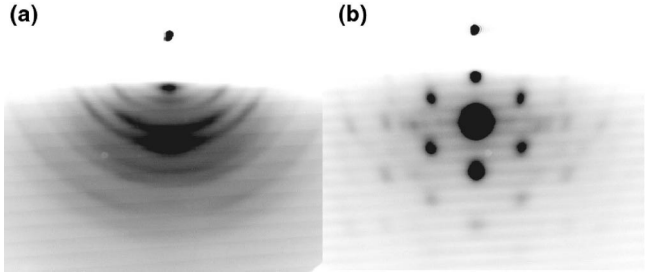


FIG. 2. RHEED images taken after growth of the $KNiF_3$ film. Except for substrate temperature, growth conditions were the same for all samples, but a variety of polycrystalline, single-crystal and two-phase bicrystalline $KNiF_3$ films were grown. An example of polycrystalline structure is shown in (a), and an example of single-crystal structure is shown in (b).

aligned at grazing incidence (about 88° from the sample normal) for a glancing-angle x-ray diffraction.

Another potassium fluoride system $Fe/KCoF_3$ has also been studied and the similarities to the present $KNiF_3$ system are noteworthy.[28] Similar to the $KNiF_3$ system, detailed analysis of x-ray-diffraction patterns for $Fe/KCoF_3$ bilayers reveal a high degree of (100) texture even for polycrystalline antiferromagnet films, with a narrow distribution of axes aligned primarily along the Fe[110] direction. A set of reflections with very low intensity indicate contributions from (110) $KCoF_3$ crystal orientations, suggesting that a small subset of the interface is uncompensated.

For all single-crystal structures of the potassium fluoride systems grown, the x-ray pattern clearly showed the $(00h)$ reflections of the GaAs substrate, plus the (001), (002), and (004) reflections of the epitaxially grown (001) films with

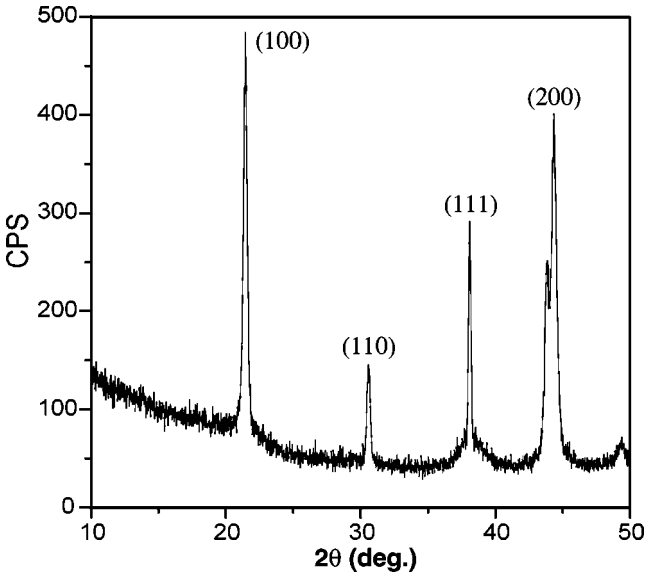


FIG. 3. X-ray (Cu-$K\alpha$ wavelength) diffractograph of a 100 nm test $KNiF_3$ film grown directly on the GaAs substrate. The incident beam was aligned at grazing incidence (about 88° from the sample normal) for a glancing-angle x-ray diffraction The spectrum was then acquired by scanning the x-ray detector through a large angle.

TABLE I. Structural parameters for $Fe/KNiF_3$ bilayers. Film thickness for the Fe and $KNiF_3$ ($t_{Fe}$ and $t_{KNiF_3}$, respectively), crystalline quality of the $KNiF_3$, and saturation magnetization are listed for each sample. In the first column, the sample-labeling scheme is introduced where S means single crystal (sc), B means two-phase bicrystalline (bc), and P means polycrystalline (poly). The first number is the ferromagnetic film thickness, and the second is the antiferromagnetic film thickness. Qualitative structure was determined from RHEED patterns. Saturation magnetization is given at 5 K and 300 K, and a ratio of these values is given in the last column. These ratios are all well in excess of 1.02 established for Fe, suggesting that a significant seed-layer magnetization appears at low temperature. Thicknesses are in nm, and saturation magnetizations $M_s$ are in emu/cm$^3$.

| Label | $t_{Fe}$ | $t_{KNiF_3}$ | $KNiF_3$ structure | $M_s$ (5 K) | $M_s$ (300 K) | $M_s$ ratio |
|---|---|---|---|---|---|---|
| S-1.4-20 | 1.4 | 20 | sc | 1950 | 1740 | 1.12 |
| B-1.5-20 | 1.5 | 20 | bc | 2040 | 1840 | 1.11 |
| B-1.4-30 | 1.4 | 30 | bc | 2020 | 1570 | 1.29 |
| P-1.6-20 | 1.6 | 20 | poly | 1930 | 1710 | 1.13 |
| P-1.7-20 | 1.7 | 20 | poly | 2050 | 1800 | 1.14 |
| P-1.9-30 | 1.9 | 30 | poly | 2210 | 1870 | 1.18 |
| P-1.9-120 | 1.9 | 120 | poly | 2060 | 1650 | 1.25 |
| P-1.4-120 | 1.4 | 120 | poly | 2030 | 1610 | 1.26 |

no visible indication of other textures. Importantly, all antiferromagnet films were grown using the same *e*-beam conditions, and all show peaks indexable to the stoichiometric compound (see Fig. 3). This indicates that decomposition of the fluoride does not occur under these growth conditions.

A total of eight samples were prepared with various film thicknesses and, in some cases, using different temperatures during $KNiF_3$ film growth in order to obtain better crystalline growth. No clear correlation between growth conditions and structure was observed, but it was possible to optimize crystalline growth of the $KNiF_3$ by adjusting substrate temperature and deposition rate. A summary of thickness parameters, antiferromagnet film structure, and saturation magnetization is given in Table I. A sample-labeling scheme is introduced as follows. Sample names begin with the letters "*S*," "*B*," or "*P*," to denote single-crystal, two-phase bicrystalline, or polycrystalline structure, respectively, in the $KNiF_3$ film. The two subsequent numbers denote the thicknesses of the Fe and $KNiF_3$, respectively, in units of nm. The magnetization measurements and seed-layer contributions will be described in the next section.

## III. MAGNETIC MEASUREMENTS

Magnetic measurements were made using a Quantum Design SQUID magnetometer. For zero-field-cooled measurements, the samples were first ac demagnetized at room temperature. For field-cooled measurements, the samples were cooled in a 20 kOe field before collecting magnetization loop data. Loops were measured along the in-plane easy and in-plane hard anisotropy axes of the Fe film. A sketch showing the orientation of the applied field relative to the expected

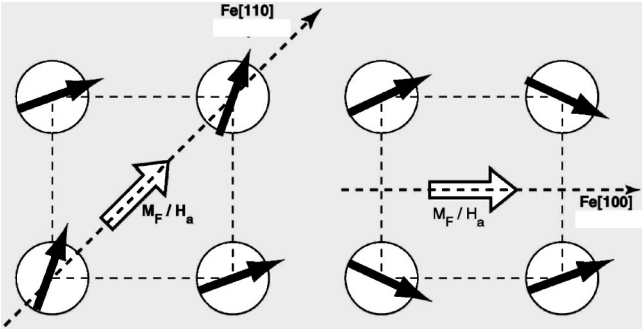


FIG. 4. Schematic diagram showing the expected spin structure at the ferromagnet-antiferromagnet interface, for in-plane magnetization measurements along an easy Fe anisotropy axis (a) and along a hard Fe anisotropy axis (b). Note that magnitude of the canting angles has been greatly exaggerated for clarity. The actual canting angles should be much smaller than those depicted here.

spin structure at the ferromagnet-antiferromagnet interface is given in Fig. 4 (note that magnitude of the canting angles has been greatly exaggerated for clarity). The SQUID solenoid was also quenched prior to hysteresis loop measurements, to remove the remanence field of the solenoid. A number of studies were made in order to investigate the variety of features observed in the magnetization loops. The results are presented below and organized according to features. First, a discussion of magnetic hysteresis effects introduced by the seed layer is presented, followed by a definition of bias shifts and coercive fields. Temperature dependencies are next discussed in relation to possible origins of the bias shift and coercivity.

### A. Hysteresis and the seed layer

An example of a magnetization loop is shown in Fig. 5 for sample P-1.7-20 field cooled down to 15 K. The loop shown in Fig. 5(a) is typical of results found for most of the samples in terms of its general features and magnitudes for the coercive fields. As can be seen, there are several unusual features in the loop shown in Fig. 5(a). The coercivities, defined as $H_{c1}$ for the reverse direction and $H_{c2}$ for the forward direction, are not symmetrical with respect to $H=0$. The asymmetry of the coercivities indicates a bias of the entire magnetization loop.

Perhaps the most striking features are the large tails on the magnetization as the field approaches saturation in the positive and negative directions. This contribution is due to the seed layer. Ideally the seed layer should not be ferromagnetic after annealing. Instead, it appears to act as a superparamagnetic element in the sample which contributes to the total magnetization at temperatures near room temperature, and as a ferromagnetic element at low temperatures. This can be seen from the saturation magnetizations listed in Table I, which for most samples are in excess of established values for Fe at 5 K and 300 K (1750 erg/cm$^3$ and 1715 erg/cm$^3$, respectively). However, these values are consistent with the appearance of up to 0.6 nm of Fe from the seed layer at low temperatures. In some samples, up to 0.3 nm of ferromagnetic seed-layer contributions persist up to room temperature. There is insufficient information to determine whether these elements in the seed layer contributing to magnetization form a contiguous film or a random collection of small ''islands.''

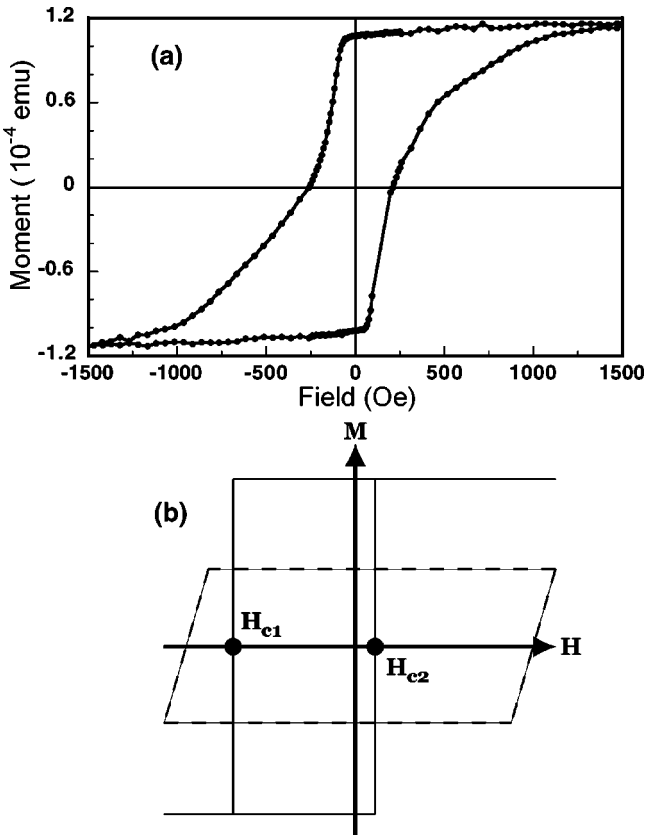


FIG. 5. The magnetization loop for sample P-1.7-20 when field cooled to 15 K is shown in (a). The applied field is along the Fe film [110] direction, an easy magnetization direction for the ferromagnet. Note the large magnetization tail at positive and negative saturation fields. This tail is due to superparamagnetic elements originating in the seed layer. A sketch of how the seed layer creates the tail is shown in (b).

Evidence for this conjecture was obtained by noting that the tails are symmetrical with respect to $H=0$. It is also significant that magnetization loops at 77 K cross-checked by longitudinal magneto-optic Kerr-effect (MOKE) magnetometry do not show any sign of these tails, since the HeNe laser beam used in our MOKE apparatus is unable to penetrate the thick Ag film. The contribution from the seed layers can be thought of as a superposition of a square shifted loop associated with Fe in the bilayer and a wide, rounded loop representing a random distribution of ferromagnetic particles. This superposition is sketched in Fig. 5 where the dashed lines represent the contribution from the seed layer.

The seed layer is magnetically isolated from the bilayers by the Ag layer and does not affect exchange bias or coercivity. Determination of the bias shift and a measure of coercivity can therefore be determined from magnetization loops by measuring the intercepts of the loop on the applied field axis. This is denoted $H_{c1}$ and $H_{c2}$ in Fig. 5.

### B. Coercivity and bias shifts

Features associated with the magnetization loops are now examined. First, the difference between $H_{c1}$ and $H_{c2}$ in Fig. 5(a) is about 100 Oe. Antiferromagnetic resonance measurements on $KNiF_3$ at 4.2 K indicate that the anisotropy of the antiferromagnet in bulk form is on the order of 80 Oe (Ref. 11) and magnetic anisotropy of bulk Fe is on the order of 500 Oe. The width of the curve does not therefore appear to correlate with antiferromagnet anisotropies, nor does it seem to correlate directly with anisotropies in the ferromagnet. Instead, magnetization processes involving domain nucleation, pinning, or wall motion within the heterostructure must be involved.

The existence of a bias shift is a curious feature of this epitaxially grown system since the interface should be mainly compensated. A first question to address is how a nonzero torque can be transmitted from the ferromagnet to the antiferromagnet through a compensated interface. A possible mechanism is through some form of spin-flop coupling. The antiferromagnetic exchange field at low temperatures is on the order of $10^5$ times larger than the anisotropy field.[11] At the interface between the ferromagnet and antiferromagnet, the local exchange and anisotropy fields can be expected to have a similar ratio and possess comparable magnitudes to those in bulk material. An estimate of the spin-flop field is given by $H_{sf}=\sqrt{2H_eH_a}$ where $H_e$ is the $KNiF_3$ exchange field and $H_a$ is the anisotropy field. This gives a $H_{sf}$ on the order of 1 kOe. A reasonably strong interface exchange coupling would therefore likely result in a considerable canting of $KNiF_3$ spins near the interface.

At this point it should be noted that the saturating fields used in this experiment could conceivably be larger than the spin-flop field. If true, there can be significant consequences for the observed bias field, angular bias field dependence, and coercivity.[29] Bicrystalline and polycrystalline samples in particular may involve complex magnetization processes during a hysteresis loop measurement as the applied field is taken through the spin-flop field. The reason is that spin flop depends on the interlayer exchange field introduced by the ferromagnet, the applied magnetic field, and the orientation of these fields relative to the direction of the local antiferromagnetic uniaxis. This means that spin flop is likely to be nonuniform across the interface during a magnetization loop measurement. A complete study of these effects in the $KNiF_3$ system would be very interesting, but beyond the scope of the present work. In this initial study the saturating field is set well above the estimated spin-flop field in order to at least provide a consistent reference point for magnetization measurements.

The net interface moment on the antiferromagnet side due to the canted state provides a means by which a torque on antiferromagnetic spins can be generated, but there remains a problem of understanding the existence and magnitude of the hysteresis loop shift. A bias field can be defined as $H_b=\frac{1}{2}(H_{c2}+H_{c1})$. From the loop shown in Fig. 5(a), $H_b$ is about 50 Oe. A summary of bias fields measured by SQUID magnetometry is included in Table II. Even though it is possible for the ferromagnet to exert a torque on the antiferromagnet via a spin-flopped interfacial spin configuration, it has been shown by several authors that a spin-flop configuration is not stable without the existence of large in-plane anisotropies or interface imperfections capable of pinning antiferromagnet domain configurations.[16,18,22,30]

TABLE II. Measured bias fields for the Fe/$KNiF_3$ bilayers, normalized as $\Delta E=H_bM_st_{Fe}$. For each sample, the bias fields for field cooling along different Fe crystallographic directions are listed. The samples are labeled as in Table I, and bias fields are reported at two different temperatures along three different directions. Field-cooling directions are indicated by "EFC" for cooling along the easy direction [001], "$HFC_1$" for cooling along the hard direction [110], and "$HFC_2$" for cooling along the hard direction $[\bar{1}10]$. The unit of $\Delta E$ is $10^{-4}$ erg/cm$^2$.

| Label | EFC 5 K | EFC 25 K | $HFC_1$ 5 K | $HFC_1$ 25 K | $HFC_2$ 5 K | $HFC_2$ 25 K |
|---|---|---|---|---|---|---|
| S-1.4-20 | 1.4 | 0.3 | 2.0 | 0.4 | 1.7 | 0.6 |
| B-1.5-20 | 1.4 | 0.7 | 1.3 | 0.6 | | |
| B-1.4-30 | 2.1 | 1.0 | 2.6 | 1.2 | 2.3 | 1.1 |
| P-1.7-20 | 4.6 | 0.3 | 6.4 | 0.4 | | |
| P-1.6-20 | 0.2 | 0.0 | | | | |
| P-1.9-30 | 0.5 | 0.1 | 0.5 | 0.0 | 0.1 | 0.0 |
| P-1.9-120 | 0.9 | 0.0 | 0.3 | 0.0 | 0.5 | 0.0 |
| P-1.4-120 | 0.1 | 0.0 | 0.3 | 0.0 | 0.0 | 0.0 |

The energy required to drag the antiferromagnet through reversal scales with the thickness of the antiferromagnet. Films with thickness greater than a domain-wall length preferably form a twist rather than reverse completely. This can provide a mechanism for bias, as pointed out by Mauri *et al.*[20] and Koon,[15] provided that the anisotropy is uniaxial rather than fourfold. Even so, it is possible that uniaxial anisotropies might be present due to tetragonal distortions, possibly originating near the interface or driven by strain due to lattice mismatch.

A check on this possibility was made by examining systems with different antiferromagnetic film thicknesses. A minimum thickness estimate can be made assuming anisotropy and exchange field values on the order of the bulk values discussed above. The characteristic length of a domain wall in the $KNiF_3$ is then given by $\sqrt{H_e/H_a}$. Using published ratios of $H_e$ to $H_a$ for $KNiF_3$,[11] this length is $\approx$450 atomic planes, or 180 nm. If the exchange bias involved formation of such a twist, then a difference in the bias field should appear between samples with vastly different $KNiF_3$ film thicknesses. Samples were grown with $KNiF_3$ thicknesses of 20 nm and 120 nm, then examined for exchange bias. No clear correlation between bias and $KNiF_3$ thickness was found.

The above considerations suggest that exchange bias in this system originates from two features. First, it is reasonable to assume that interlayer exchange coupling across the interface is large enough to induce a significant deformation of antiferromagnetic spin ordering at the interface for a net magnetic moment to be induced at the interface. Furthermore, structurally it is likely that the interface is not perfect and uncompensated spins or regions of spins exist for many

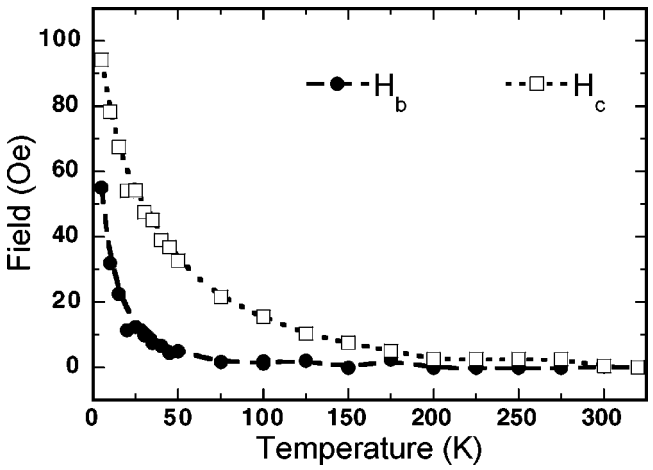


FIG. 6. The bias shift $H_b$ and coercive field $H_c$ as a function of temperature for sample S-1.4-20. Note the rapid decrease of bias shift with a blocking temperature well below $T_N$. The enhancement of Fe coercivity due to coupling with $KNiF_3$ persists up to much higher temperatures. $H_b$ and $H_c$ values were obtained from magnetization loops measured along an Fe easy anisotropy axis.

samples in this study. Even though spin-flop coupling alone may not be sufficient to produce exchange bias shifts, with both of these contributions a relatively weak exchange coupling can exist between the ferromagnet and antiferromagnet throughout a magnetization loop cycle.

Second, the magnitude of the bias shift does not appear to show any clear dependence on antiferromagnetic film thickness and therefore probably does not involve irreversible formation of a twist in the antiferromagnetic spin order. The lack of correlation between bias shift and film thickness, together with large variations of bias shift observed throughout the range of samples, would be consistent with a mechanism for bias involving domain pinning within the antiferromagnet. Evidence for this interpretation is provided in the following section through data taken at different temperatures and also from training effects described in Sec. IV.

### C. Temperature dependence

The $KNiF_3$ phase is known to retain the cubic structure[31] down to 4.2 K.[11] $KNiF_3$ is antiferromagnetically ordered below its Néel temperature $T_N$ which is estimated to be 250 K (Refs. 32 and 33) according to calorimetric methods or 270 K (Refs. 32 and 34) from magnetic measurements. Measurements were made over this temperature range, and results for bias field and hysteresis loop width were obtained for each sample listed in Table I. An example is shown for sample S-1.4-20 in Fig. 6. The bias field has been defined previously as the average of $H_{c1}$ and $H_{c2}$. The coercive field $H_c$ is defined as the difference $\frac{1}{2}(H_{c2}-H_{c1})$.

As can be seen in Fig. 6, and typical of all samples studied, the bias field shift decreases rapidly as a function of temperature and disappears at a temperature well below the ordering temperature $T_N$ of the antiferromagnet. The low blocking temperature is difficult to understand unless one supposes some sort of domain pinning process in the antiferromagnet which becomes unstable at relatively low temperatures. It is interesting to note that antiferromagnetic resonance studies show anomalous resonant absorption below the same approximate blocking temperature.[35,11] However, this feature does not appear to be magnetic in origin,[11] nor does it appear to be correlated with magnetostriction.[36]

TABLE III. Measured coercivity for $Fe/KNiF_3$ bilayers. For each sample, the widths of the magnetization loop for field cooling along different Fe crystallographic directions are listed. The samples are labeled as in Table I, and coercive fields are reported at two different temperatures along three different directions. Field-cooling directions are indicated by "EFC" for cooling along the easy direction [001], "$HFC_1$" for cooling along the hard direction [110], and "$HFC_2$" for cooling along the hard direction $[\bar{1}10]$. Coercive fields are also given for a single-crystal Fe film covered by Au, which was codeposited during growth of sample P-1.7-20. Field units are Oe.

| Label | EFC 5 K | EFC 25 K | $HFC_1$ 5 K | $HFC_1$ 25 K | $HFC_2$ 5 K | $HFC_2$ 25 K |
|---|---|---|---|---|---|---|
| Fe | 151 | 60 | 149 | 66 | | |
| P-1.7-20 | 321 | 235 | 442 | 249 | | |
| S-1.4-20 | 94 | 54 | 155 | 102 | 96 | 64 |
| P-1.6-20 | 45 | 22 | | | | |
| B-1.5-20 | 296 | 229 | 318 | 250 | | |
| P-1.9-30 | 79 | 44 | 65 | 32 | 75 | 34 |
| P-1.9-120 | 73 | 40 | 44 | 33 | 59 | 40 |
| P-1.4-120 | 75 | 55 | 108 | 74 | 65 | 55 |
| B-1.4-30 | 115 | 88 | 103 | 80 | 99 | 73 |

As discussed above, the origin of anisotropies that could pin the ferromagnet and create coercivity is unclear for this system. Possible uniaxial anisotropy contributions to the coercive and bias fields should appear when comparing data taken along the principal in-plane axes associated with the fourfold anisotropy of the ferromagnet. Results for $H_b$ and $H_c$ determined for all samples are listed in Tables II and III, from hysteresis loop measurements at different temperatures and for field cooling along different Fe crystallographic directions.

Measurements were made for cooling along the Fe[100] easy anisotropy direction, and along two hard directions, Fe[110] and Fe$[\bar{1}10]$ directions. Field cooling along the Fe easy direction is denoted "EFC." Field cooling along the Fe hard directions is denoted "$HFC_1$" and "$HFC_2$," respectively. These directions coincide with the anisotropy axes of $KNiF_3$. The data suggest that the $KNiF_3$[100] and $KNiF_3$[010] directions are not equivalent as sources of pinning for the ferromagnet, possibly due to the tetragonal lattice distortion that breaks the exact fourfold symmetry of the $KNiF_3$ surface. There is no clear correlation visible between cooling direction and either bias or coercivity.

Included in Table III are results for a single Fe film grown on a silver template. Examination of hysteresis for this single film revealed a strong temperature dependence of coercivity. This feature is due to domain formation and wall motion near $H=0$. Domain nucleation and wall motion are sensitive to the temperature dependence of the ferromagnet anisotropy and ferromagnetic domain-wall pinning at defects. Observa-

tion of magnetic domains in the Fe film by Kerr microscopy confirms domain-wall nucleation and propagation as the dominant mechanism of reversal during hysteresis loop measurements.

There is a wide spread of values for low-temperature coercive field across the range of samples. There is clearly some relation between antiferromagnetic ordering below $T_N$ and measured coercivities, but it is difficult to say whether there is an appreciable enhancement of coercivity due specifically to irreversible domain-wall processes in the antiferromagnet. It would seem in fact that the coercivity and bias shifts are dominated largely by domain formation and domain-wall motion in the ferromagnet. We note that the coercivity is very narrow above $T_N$ at 300 K, and independent of applied field orientation. This certainly indicates domain formation within the ferromagnet, and is similar to behavior observed for single Fe films grown for reference.[25]

In this interpretation, coupling with the antiferromagnet enters by modifying, to some extent, domain-wall pinning fields and stabilization of domain states in the ferromagnet. Temperature dependence of the coercive and bias fields then appear through thermally activated processes associated with the modified pinning centers and activation energies.

## IV. TRAINING EFFECTS

Hysteresis and coercivity exist because there are multiple stable and metastable magnetic configurations available to the system. This is sometimes described by an energy landscape in which each magnetic configuration corresponds to a particular energy, and stable configurations are separated by energy barriers. Thermal fluctuations can lead to changes of the system from one configuration to another. The rate at which these changes occur depends on the height of the energy barrier relative to the magnitude of the energy involved in the thermal fluctuation.

These types of processes are often described using concepts from thermal activation theory which has been formulated for ferromagnetic systems by a number of authors.[37–39] The problem for exchange bias systems was first examined experimentally by Schlenker[40] and one of the first models for the phenomena was presented by Fulcomer and Charap.[41] Recent experimental and theoretical work for thermal activation and rate-dependent phenomena has also appeared.[42–45]

Thermal activation can involve a number of magnetization processes including coherent reversal of small particles, nucleation, and growth of domains, and depinning of domains and domain walls. Because the relative height of effective energy barriers separating different magnetic configurations depends on applied magnetic field, the probability that a thermal event will occur depends on applied magnetic field as well as temperature. It is therefore possible to experimentally probe thermally activated magnetic processes using magnetization experiments in which the applied field is varied. Two types of experiments have been performed in which thermal activation of magnetization processes has been explored. The first type involved creating successive magnetization loops by cycling through the field ranges several times and noting changes in the coercive and bias fields. The second type is referred to as a thermal pulse experiment and was done by going part of the way through a magnetization loop, fixing the applied field and changing the temperature for some time interval, and then completing the loop at the original temperature.

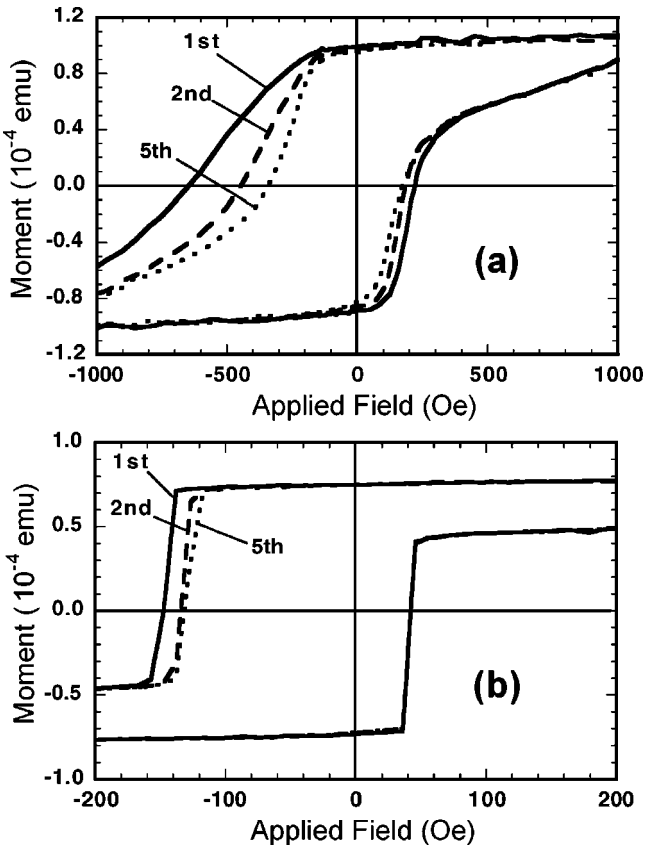


FIG. 7. Cycled magnetization loops at 20 K for bilayer structures P-1.7-20 and B-1.4-30 with antiferromagnetic film thickness 20 nm (a), and 30 nm (b). The loops were made at a constant temperature of 20 K. The reverse field coercivity changes during the initial cycles, and equilibrium is reached after about five consecutive loops. Note in each case the long magnetization tail is due to the seed layer.

### A. Field cycling

Results of repeated cycling of the applied magnetic field are shown in Fig. 7 for samples with two different antiferromagnetic film thicknesses (P-1.7-20 and B-1.4-30). In both cases the samples were first field cooled to 4.2 K before beginning the magnetization loops. Loops were made consecutively at a constant temperature of 20 K. The field was changed at the same rate throughout the cycling processes. The coercivity in the reverse field direction, $H_{c1}$, is changed by the cycling process, but the forward loop coercivity $H_{c2}$ is not strongly affected.

It is significant that cycling only appears to affect coercivity for one branch of the magnetization loop. A steady state is reached when, for consecutive loops, there are only two unique values for $H_{c1}$ and $H_{c2}$, regardless of the number of field cycles. Along a given branch of the loop, changes in

the value of $H_c$ along that branch signal irreversible changes of the magnetization configuration. These changes involve some type of thermal activation over energy barriers associated with domain stability, originating either in the ferromagnet or in the antiferromagnet.

One set of barriers appears to govern domain nucleation and wall movement in the ferromagnet. The rate of magnetization appears to depend on the magnitude of the applied field but a weak temperature dependence to the rates observed in the experiments suggests that effective pinning fields created by the antiferromagnet play a small role. At least in this regard, the formation of domain structure within the ferromagnet appears to be dominated by magnetostatic effects, with pinning of ferromagnetic domains and walls strongly influenced by energy barriers associated primarily with the ferromagnetic film.

The antiferromagnet itself is only indirectly sensitive to the applied field. Exchange coupling across the interface leads to the possibility for spin flop at the antiferromagnet interface, as discussed earlier, which then makes the antiferromagnet sensitive to the orientation of the ferromagnet magnetization. The interlayer exchange coupling with the ferromagnet can act to modify and create energy barriers governing the stability of domains within the antiferromagnet. These barriers may be strongly dependent on the orientation of the ferromagnet magnetization, and it is these barriers that most strongly affect the bias shift. It is likely that the barriers to domain growth and wall motion in the antiferromagnet are proportional in magnitude to the unidirectional anisotropy, as discussed by Soeya *et al.*[46] In this case, the barriers will be strongly associated with interface structure and possible frustration induced on the ferromagnet through interlayer coupling to different regions in bicrystalline and polycrystalline samples.

The fact that field cycling appears to affect $H_{c1}$ more strongly than $H_{c2}$ is suggestive of thermal activation in the ferromagnet being dominant in the field-training response. Domains in the antiferromagnet may be switching due to thermal activation along each branch of the loop. The number of antiferromagnet reversals ought to be the same on either branch because it is only sensitive to the ferromagnet magnetization, and this has the same magnitude in both directions of the field sweep. Regions of the ferromagnet which are not strongly biased experience a different magnitude of field during the forward and reverse branches, since the loop is offset from $H=0$. The number of thermally activated reversals in this set of weakly biased regions will be greater for the reverse branch of the loop where the field magnitude is larger. Any associated changes in the antiferromagnet domains would therefore be larger near $H_{c1}$ compared to $H_{c2}$. Repeated cycling finally brings the populations of reversed and unreversed antiferromagnetic domains into equilibrium, after which $H_{c1}$ and $H_{c2}$ are independent of the number of field cycles. The steady-state bias field is in fact nonzero in Fig. 7, and is reached after about five cycles of the applied field.

### B. Thermal pulse response

If the above argument explaining cycling is true, then it should be possible to affect the configuration of the antiferromagnet by thermal activation independently of the ferromagnet. Consider what happens after first cooling the sample in a large positive applied field and then applying a field in the negative direction large enough to saturate the ferromagnet. If bias exists, field cooling has aligned regions in the antiferromagnet preferentially with the ferromagnet according to the field-cooling direction. At any finite temperature with the ferromagnet aligned away from the field-cooling direction, there is some finite probability that some regions of the antiferromagnet will reverse into a low-energy direction. The time needed for a significant number of these events to occur depends on the temperature.

A feasible experiment is thus to saturate the ferromagnet in a direction opposite the field-cooled direction at a low temperature, and then briefly increase the temperature to facilitate some number of thermally activated reversals. During application of this thermal pulse, the increased temperature will cause some fraction of domains in the antiferromagnet to reorient with respect to the ferromagnet. In principle it should even be possible to reverse the direction of the bias in this manner, by either raising the temperature above $T_N$ or simply waiting long enough at a temperature below $T_N$ until thermal fluctuations reorient the majority of domains in the antiferromagnet into the new direction. Note that both coercivity fields should change in such an experiment.

This idea was tested by sweeping magnetization loops in the following manner: A sample was first field cooled in $+20$ kOe from 300 K to 4.2 K. A single hysteresis loop was then swept out between $+4$ kOe and $-4$ kOe. A field of $-4$ kOe was applied, during which the sample was warmed up to a target temperature and then immediately cooled to the original temperature of 4.2 K. The sample's temperature versus time profile takes the form of a thermal pulse of height $T_{max}$. A new hysteresis loop was acquired starting at $+4$ kOe. The effect of various pulse ''heights'' was investigated in this manner by repeating this process up to different values of $T_{max}$. The warming and cooling process associated with each thermal pulse takes about 30 min.

Results are shown in Fig. 8 for sample B-1.4-30. The plot represents data taken during a sequence wherein the target temperature was increased for each consecutive pulse. The loop width remains constant but the center shifts over to the right. A thermal pulse up to 100 K was sufficient to completely reverse the bias field, despite being well below $T_N$. The dependence of the bias field on pulse temperature during the sequence is shown in Fig. 9.

The change in bias field without significant change of the loop width in this experiment is consistent with the two sets of energy barriers as suggested above. Since a warming and cooling cycle was completed at a large negative $M_s$, the configurations of domains in the ferromagnet are unaffected by the thermal pulses. However, domains in the antiferromagnet experience effective fields through the interface exchange coupling to the ferromagnet that involve similar numbers of thermally activated processes during each branch of the magnetization loop. Therefore, unlike the field-cycling experiment, both $H_{c1}$ and $H_{c2}$ shift simultaneously during the pulse sequence while leaving the width of the loop largely unchanged.

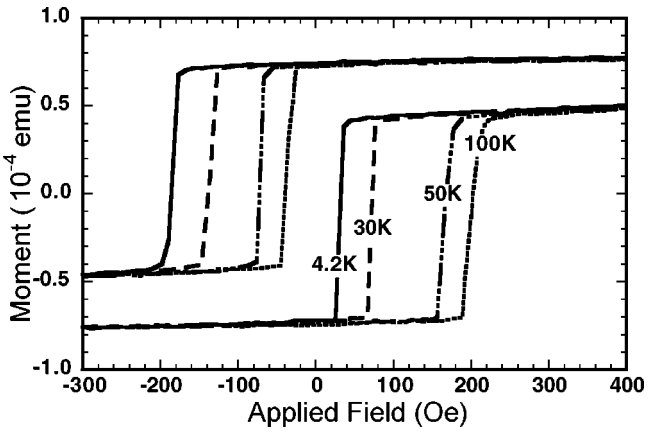


FIG. 8. Magnetization loops for B-1.4-30 at 4.2 K, after subjecting the sample to thermal pulses of magnitude $T_{max}$. Note that both $H_{c1}$ and $H_{c2}$ fields change in response to the thermal pulses. A thermal pulse of 100 K is sufficient to completely reverse the bias direction.

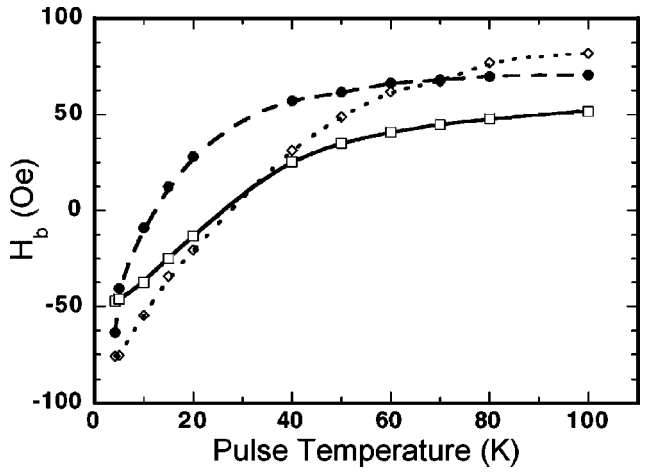


FIG. 9. The variation of the bias field $H_b$ for samples with single-crystal $KNiF_3$ films as a function of thermal pulse magnitude $T_{max}$. The filled circles are for sample S-1.4-20, the open squares are for sample B-1.5-20, and the open diamonds are for B-1.4-30. All samples were field cooled in the positive direction and thermal pulses were applied at negative saturation. The sequence of thermal pulses follows the description in the text.

## V. SUMMARY

A model exchange bias system was prepared by MBE and examined using both structural and magnetic characterization techniques. The system consists of the antiferromagnet $KNiF_3$ grown epitaxially on single-crystal Fe. There exists a good lattice match between the Fe and $KNiF_3$ films, with individual grains of the $KNiF_3$ showing well-defined cubic structure and strong overall (100) texture in plane. Both films have the principal [001] axis directed out of plane. Single-crystal, two-phase single-crystal and polycrystalline $KNiF_3$ films could be obtained simply by varying the substrate temperature during deposition. A small exchange bias field was determined for several samples even though the $Fe/KNiF_3$ interface should be compensated.

Magnetization processes in the ferromagnet were shown to involve domain formation and growth and the antiferromagnet appears to affect the ability of domains in the ferromagnet to grow. Field-cycling experiments revealed evidence for separate thermal activation processes in both the ferromagnet and antiferromagnet. Field cooling results in a predominance of domain orientations in the antiferromagnet relative to the ferromagnet that defines a bias field direction. Field cycling was found to affect only one branch of the magnetization loop, and could be explained by a distribution of fields acting on the ferromagnet. This feature may be related to asymmetries observed in magnetization processes in other systems.[47–49]

In a different type of training experiment, thermal pulses were used to demonstrate the existence of thermal activation energies associated with the antiferromagnet processes responsible for bias. It was possible to completely reverse the bias direction through application of a temperature pulse well below $T_N$, without significant modification of the magnetization loop width.

The evidence for thermally driven magnetization processes within the antiferromagnet, together with the observation of exchange bias shifts despite mainly compensated interfaces in this system, suggests that the bias is controlled by interface local effective fields acting on spins in the antiferromagnet. Weak exchange bias shifts were observed with a blocking temperature well below the antiferromagnetic ordering temperature, and did not seem to be correlated with antiferromagnetic film thickness. This is consistent with the idea of pinning fields acting mainly through the interface.

A spin-flop canting of antiferromagnet spins is expected, and whereas this may not be sufficient to account for exchange bias shifts, the persistence of coercivity up to the ordering temperature of the $KNiF_3$ is consistent with the idea of perpendicular coupling as observed in other experimental results taken from compensated CoO/NiFe as reported by Gökemeijer *et al.*[50] The interface in the $KNiF_3$ system appears to be locally of high quality, but there is definitely evidence in many samples of bicrystalline and polycrystalline growth. As discussed and observed by Hochstrat, *et al.*,[51] structural imperfections and disorder at the interface may lead to training effects in single-crystal structures. The observation of training effects originating from thermal activation processes within the $KNiF_3$ is therefore also consistent with the idea that bias shifts can exist due to frustration of the ferromagnet via coupling across regions of the interface with different structure as suggested by Fitzsimmons *et al.*[52]

## ACKNOWLEDGMENTS

L.M. and Z.C. acknowledge support by the National Science Foundation (Grant No. DMR-0303563) and the Research Corporation (Grant No. CC4619). L.W. and R.L.S. acknowledge support by the Australian Research Council (Discovery Grant, IREX and IPRS).

*Electronic address: stamps@physics.uwa.edu.au

[1] W.H. Meiklejohn and C.P. Bean, Phys. Rev. **102**, 1413 (1956).
[2] W.H. Meiklejohn and C.P. Bean, Phys. Rev. **105**, 904 (1957).
[3] I.S. Jacobs and C.P. Bean, in *Magnetism*, edited by G.T. Rado and H. Suhl (Academic Press, New York, 1963), Vol. 3, pp. 271–350.
[4] J.S. Kouvel, J. Phys. Chem. Solids **24**, 795 (1963).
[5] J. Nogués and I.K. Schuller, J. Magn. Magn. Mater. **192**, 203 (1999).
[6] A.E. Berkowitz and K. Takano, J. Magn. Magn. Mater. **200**, 552 (1999).
[7] M. Kiwi, J. Magn. Magn. Mater. **234**, 584 (2001).
[8] R.L. Stamps, J. Phys. D **33**, R247 (2000).
[9] G. Ju, A.V. Nurmikko, R.F.C. Farrow, R.F. Marks, M.J. Carey, and B.A. Gurney, Phys. Rev. B **58**, 11 857 (1998).
[10] F. Nolting *et al.*, Nature (London) **405**, 767 (2000).
[11] H. Yamaguchi, K. Katsumata, M. Hagiwara, M. Tokunaga, H.L. Liu, A. Zibold, D.B. Tanner, and Y.J. Wang, Phys. Rev. B **59**, 6021 (1999).
[12] K. Hirakawa, T. Hashimoto, and K. Hirakawa, J. Phys. Soc. Jpn. **16**, 1934 (1961).
[13] M.E. Lines, Phys. Rev. **164**, 736 (1967).
[14] M. Safa and B.K. Tanner, Philos. Mag. B **37**, 739 (1978).
[15] N.C. Koon, Phys. Rev. Lett. **78**, 4865 (1997).
[16] T.C. Schulthess and W.H. Butler, Phys. Rev. Lett. **81**, 4516 (1998).
[17] R.E. Camley, B.V. McGrath, R.J. Astalos, R.L. Stamps, J.-V. Kim, and L. Wee, J. Vac. Sci. Technol. A **17**, 1335 (1999).
[18] M. Kiwi, J. Mejía-López, R.D. Portugal, and R. Ramírez, Appl. Phys. Lett. **75**, 3995 (1999).
[19] P. Miltényi, M. Gierlings, J. Keller, B. Beschoten, G. Güntherodt, U. Nowak, and K.D. Usadel, Phys. Rev. Lett. **84**, 4224 (2000).
[20] D. Mauri, H.C. Siegmann, P.S. Bagus, and E. Kay, J. Appl. Phys. **62**, 3047 (1987).
[21] K. Takano, R.H. Kodama, A.E. Berkowitz, W. Cao, and G. Thomas, Phys. Rev. Lett. **79**, 1130 (1997).
[22] J.-V. Kim, R.L. Stamps, B.V. McGrath, and R.E. Camley, Phys. Rev. B **61**, 8888 (2000).
[23] B.V. McGrath, R.E. Camley, L. Wee, J.-V. Kim, and R.L. Stamps, J. Appl. Phys. **87**, 6430 (2000).
[24] A. Chelkowski, P. Jakubowski, D. Kraska, A. Ratuszna, and W. Zapart, Acta Phys. Pol. A **47**, 347 (1975).
[25] L. Wee, R.L. Stamps, Z. Celinski, and D. Skrzypek, J. Appl. Phys. **89**, 7555 (2001).
[26] L. Wee, R.L. Stamps, Z. Celinski, L. Malkinski, and D. Skrzypek, J. Magn. Magn. Mater. **240**, 270 (2002).
[27] J.M. van Hove, C.S. Lent, P.R. Pukite, and P.I. Cohen, J. Vac. Sci. Technol. B **1**, 741 (1983).
[28] L. Malkinski, T. OKeevan, R. Camley, Z. Celinski, J. He, W. Zhou, M. Hecker, C.M. Schneider, J. Szade, and D. Skrzypek, J. Vac. Sci. Technol. **21**, 1162 (2003).
[29] J. Nogués, L. Morellon, C. Leighton, M.R. Ibarra, and I.K. Schuller, Phys. Rev. B **61**, R6455 (2000).
[30] J.-V. Kim and R.L. Stamps, Appl. Phys. Lett. **79**, 2785 (2001).
[31] V. Scatturin, L. Corliss, N. Elliot, and J. Hastings, Acoust. Phys. **14**, 19 (1961).
[32] K. Hirakawa, K. Hirakawa, and T. Hashimoto, J. Phys. Soc. Jpn. **15**, 2063 (1960).
[33] C. Deenadas, H.V. Keer, R.V.G. Rao, and A.B. Biswas, Indian J. Pure Appl. Phys. **5**, 147 (1967).
[34] Z. Celinski and D. Skrzypek, Acta Phys. Pol. A **65**, 149 (1984).
[35] P.L. Richards, J. Appl. Phys. **34**, 1237 (1963).
[36] D.G. Money, D.M. Paige, W.D. Corner, and B.K. Tanner, J. Magn. Magn. Mater. **15-18**, 603 (1980).
[37] R. Street and J.C. Woolley, Proc. Phys. Soc., London, Sect. A **62**, 562 (1949).
[38] L. Néel, Ann. Geophys. (C.N.R.S.) **5**, 99 (1949).
[39] J.W.F. Brown, Phys. Rev. **130**, 1677 (1963).
[40] C. Schlenker and D. Paccard, J. Phys. (Paris) **28**, 611 (1967).
[41] E. Fulcomer and S.H. Charap, J. Appl. Phys. **43**, 4190 (1972).
[42] A.M. Goodman, K. O'Grady, M.R. Parker, and S. Burkett, J. Magn. Magn. Mater. **193**, 504 (1999).
[43] R.L. Stamps, Phys. Rev. B **61**, 12 174 (2000).
[44] M.D. Stiles and R.D. McMichael, Phys. Rev. B **63**, 064405 (2001).
[45] T. Hughes, K. O'Grady, H. Laidler, and R.W. Chantrell, J. Magn. Magn. Mater. **235**, 329 (2001).
[46] S. Soeya, T. Imagawa, K. Mitsuoka, and S. Narishige, J. Appl. Phys. **76**, 5356 (1994).
[47] M.R. Fitzsimmons, P. Yashar, C. Leighton, I.K. Schuller, J. Nogués, C.F. Majkrzak, and J.A. Dura, Phys. Rev. Lett. **84**, 3986 (2000).
[48] I.N. Krivorotov, C. Leighton, J. Nogués, I.K. Schuller, and E.D. Dahlberg, Phys. Rev. B **65**, 100402(R) (2002).
[49] V.I. Nikitenko, V.S. Gornakov, A.J. Shapiro, R.D. Schull, K. Liu, S.M. Zhou, and C.L. Chien, Phys. Rev. Lett. **84**, 765 (2000).
[50] N.J. Gökemeijer, R.L. Penn, D.R. Veblen, and C.L. Chien, Phys. Rev. B **63**, 174422 (2001).
[51] A. Hochstrat, C. Binek, and W. Kleemann, Phys. Rev. B **66**, 092409 (2002).
[52] M.R. Fitzsimmons *et al.*, Phys. Rev. B **65**, 134436 (2002).